In-Situ Measurement of Clipless Cycling Pedal Floating Angles (P51)

Yvan Champoux[1], Daniel Paré, Jean-Marc Drouet, Denis Rancourt

Topics: Bicycle, Measurement Systems.

Abstract: In cycling sports, clipless pedals are used by athletes and dedicated cyclists to attach the shoe to the pedal because this allows efficient energy transfer to the bike. Most clipless pedals now offer a degree of freedom (float) to the shoe around an axis normal to the pedal surface. This feature was originally introduced in an attempt to reduce knee injuries due to overuse. Most studies reporting on the influence of the clipless pedal floating angle on knee injuries have been carried out under laboratory conditions and little is known about the use of the float in real road conditions. This paper is an evaluation of the design and accuracy of a new apparatus that can measure the in-situ clipless cycling pedal floating angle. A high-sensitivity sensor that can measure magnetic field orientation is embedded in a commercial pedal. Small magnets temporarily clipped onto the cleat create the required magnetic field around the sensor. This measurement technology eliminates the need for a physical connection between the sensor and the shoe, thus allowing the pedal to be used normally. Static calibration and a subsequent accuracy check revealed that the angle measurement uncertainty was found to be within a range of ±0.25º with an hysteresis of less than 1% Full Scale. Typical in-situ sample floating angle measurements are included to demonstrate the ability of the instrument to provide useful information.

Keywords: Measurement, clipless pedals, floating angle, cycling.

1- Introduction

In cycling sports, 41% of overuse injuries/complaints occur at the knee. Several studies have investigated potential knee injury mechanisms in cycling (Ericson *et al.* 1984) (Ruby, Hull and Hawkins, 1992) (Ruby *et al.* 1992) (Bailey *et al.* 2003). A clipless pedal was first commercialized by LOOK Cycle in 1984. This type of pedal attaches the shoe to the pedal and allows efficient energy transfer to the bike. Modifications of the clipless pedal have included the introduction of an additional degree of freedom to the shoe (float) around an axis normal to the pedal surface in such a way that the foot's internal

1. Mechanical Engineering Department, VélUS Group, Université de Sherbrooke, Sherbrooke (Quebec) Canada J1K 2R1
E-mail: Yvan.Champoux,Daniel.Pare,Jean-Marc.Drouet,Denis.Rancourt@USherbrooke.ca

and external rotation is allowed within a limited and set range of motion. The foot movement allowed by the float reduces pedal loads and varus/valgus knee moments (Ruby and Hull, 1993) (Boyd *et al.* 1997).

To the authors' knowledge, the studies reporting on the influence of the clipless pedal floating angle on knee injuries were carried out under laboratory conditions. Consequently, there is no information available on how cyclists actually use the floating angle in different road situations. The goal of this study was to develop and test an apparatus specially designed to provide accurate and reliable monitoring of the in-situ time variation of the floating angle of commercially available clipless pedals. The apparatus needed to be lightweight, small, easy to use and to not perturb the natural motion of the foot while allowing the cyclist to easily clip in and out.

The floating allowed by the two commercial pedal models selected for use in this study (LOOK KéO and LOOK PP 336) was limited to an angular rotation θ range of 9° along an axis normal to the pedal surface, as shown in Fig. 1. The floating axis is located approximately 25 mm in front of the pedal axis. The 0° mark of the floating angle corresponded to the most counter-clockwise position of the floating range as seen from above. The positive floating angle corresponded to a clockwise rotation of either the left or right shoe. Most commercial clipless pedals are generally based on the same functioning principle and use similar components. A cleat is solidly attached to the underside of the shoe. The spring loaded pedal mechanism holds the cleat solidly in place and allows the cyclist to clip in and clip out of the pedal. Most clipless pedals offer a rotational floating along the Z axis but some of them also allocate a few centimetres of freedom along the *Y* axis.

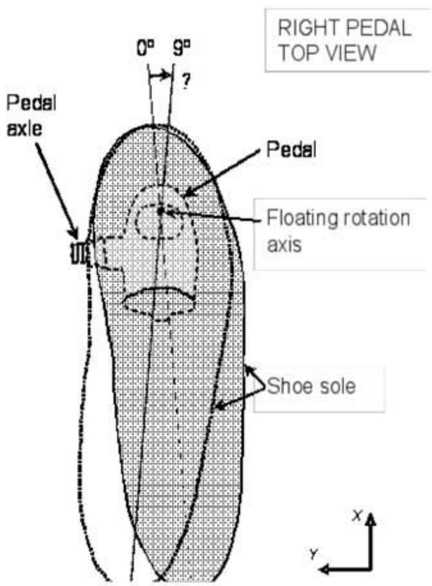

Figure 1 - Clipless pedal floating representation. View from above the right pedal. Floating is identified by a rotation θ along the floating axis in –Z direction. Floating angle θ increases with a clockwise rotation of the shoe.

Within the floating 0º-9º range, the resistance moment of the pedal along the Z axis is small and is generated by dry friction between the cleat and the pedal. To disengage the foot from the pedal, the cyclist must apply a strong moment along the Z axis to rotate the shoe beyond the resistance-free 0°-9° range up to angles of approximately –16° and +25°. Consequently, at angles of less than 0° or greater than 9° the cyclist experiences external moment loads around the Z axis.

2- Measurement system

The commercial clipless pedals were equipped with a Honeywell angular displacement sensor HMC 1501. This sensor is composed of a Wheatstone bridge and a high-resolution low-power magnetic resistance transducer that measures magnetic field angle direction with a resolution of 0.07º.

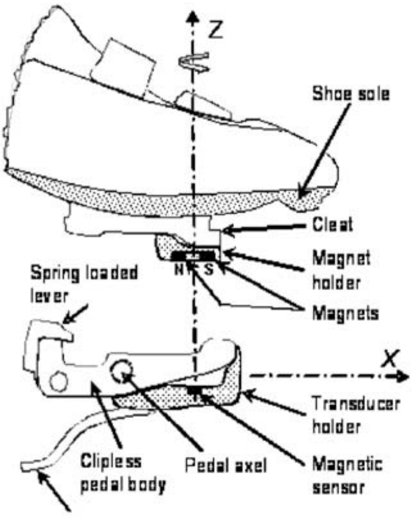

Figure 2 - Diagram of the apparatus

The bandwidth response is between 0-5 MHz. The transducer is very small and occupies a volume of only 5 mm x 4 mm x 1.2 mm. Unlike incremental encoding devices, the sensor detects absolute position and requires no indexing for proper positional output. The available full-scale output range is 120 mV for a bridge excitation of 5 V. The small transducer was held in place under the pedal with a plastic support glued to the pedal body as shown in Fig. 2. The additional weight of the device for one pedal is of the order of 80 g.

A ceramic horseshoe magnet was anchored underneath the cleat with a small aluminium holder. Magnetic north and south poles created a strong magnetic field around the sensor. The rotation of the shoe/cleat modified the magnetic field which is detected by the sensor. The sensor was aligned along the axis of rotation of the shoe/cleat. There was a gap of 4 mm between the magnets and the top surface of the sensor. An ISAAC Instruments Dual action Wheatstone bridge conditioner model MODWBD-101

(3 mV/V Full Scale) was used to supply the proper signal conditioning to the sensor. An inductive proximity probe with sufficient sensitivity to detect the passage of the crank without requiring target or reflective tape was installed on the frame. This generated a one-pulse-per-revolution synchronisation signal which was used to segment the signal and to calculate cycle averages.

A Model v7 Pro ISAAC Instruments Data Acquisition System was used to store the signals on three channels. With a sampling rate of 1 kHz and a memory capacity of 128 Mb, signals can be recorded for over 5 hours. The recorder and its battery pack were mounted on a modified Camelback® hydration pack. Small electric wires connecting the pedals to the recording system were routed along the cyclist's lower limb. The recorded data was transferred to a computer with a USB connexion for post processing.

3- Calibration

The Honeywell HMC 1501 sensor electrical voltage output ΔV is

$$\Delta V = V_s S \sin(2ø) \tag{1}$$

where V_s is the supply voltage, S is a constant determined by the material and ø is the angle between the orientation of the sensor and the magnetic field. For such a sinusoidal function at angles near 0°and for a small angle range (15°), a linear behaviour of the sensor can be assumed.

For calibration, an accurate protractor was directly attached to a cleat in place of a shoe. Floating angles and sensor outputs were simultaneously recorded and used to determine the instrument's direct sensitivity. A very good linearity was obtained (R^2=0.999) and a nominal sensitivity of 0.45 mV/V/° was measured.

Because small angle variations are measured, any unwanted relative displacement (besides the rotation related to the floating angle) between the magnet and the sensor provoked by pedal loadings would perturb the measurements. Static Loads (forces F_x, F_y, F_z; moments M_x) were individually applied to a cleat mounted on the instrument to verify the sensitivity of the measured floating angle to loads applied to the pedal. Moment M_y was not applied because it is produced by the pedal bearing friction and can thus be neglected. Moment M_z was also not considered because it is directly responsible for the floating angle variations. Using the load ranges shown in Table 1, maximum angle errors respectively for each load were measured. The total root mean square error related to pedal loads was found to be smaller than 0.25°. The hysteresis was also determined from the calibration data; it introduced a maximum error of less than 1% Full Scale. The calibration procedure was repeated at several occasions over a long period of time (more than 2 years) and the maximum variation of the sensitivity was less than 1% guarantying a good reproducibility in the measurements.

Component	Loads	
	Min	Max
F_x (N)	-180	450
F_y (N)	-360	360
F_z (N)	-1000	350
M_x (N·m)	-18	18

Table 1 - Pedal loads for the evaluation of the instrument's cross-sensitivity.

4- Sample data for the in-situ floating angle

To give examples of typical results and to demonstrate the ability of the floating angle measurement instrument, in-situ loading angles were measured in various conditions as shown in Figure 3. Each single floating cycle is described by its amplitude and angular position. As shown in Fig. 3c, the amplitude of the selected cycle (2.1°) corresponds to the peak-to-peak amplitude over the cycle. The angular position (3.5°) of the cycle corresponds to the central angular value of the cycle. A modified version of a polar plot provides an interesting global representation of a complete run, as shown in Fig. 4. Each cross denotes the amplitude (radial distance from the origin of the plot) and position (angular position) of a single cycle. The white dot in the centre of the grey square indicates the average angular position and amplitude for all the cycles under consideration. The two thin curved lines on both the left and right of the pedal polar plot indicates the zone limits within which the cyclist does not exceed the pedal floating range.

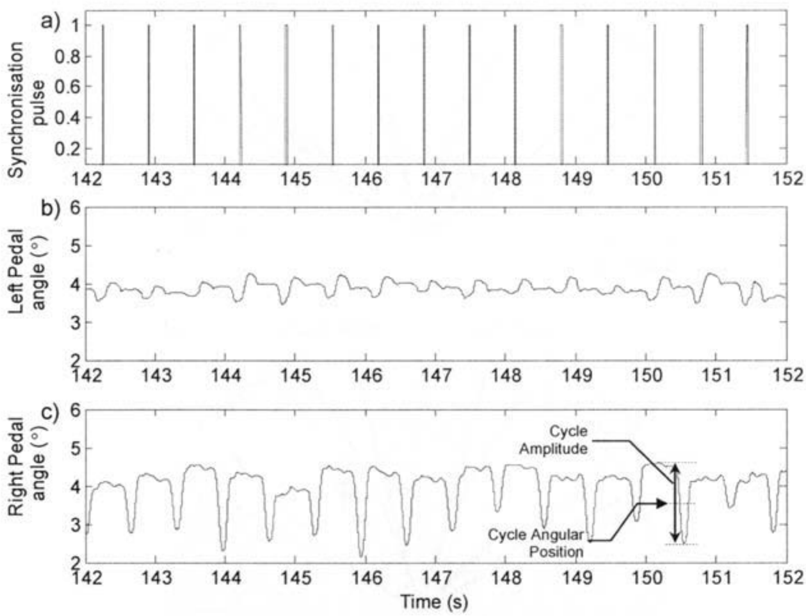

Figure 3 - Measured signals as a function of time. a) Synchronisation signals generated by the trigger signal b) Left pedal floating angle c) Right pedal floating angle.

The results in Fig 4a) show that for the cyclist being tested during flat road sitting, the right pedal floats near the centre of the available floating range. However, the results for the left pedal indicate that the cyclist consistently exceeds the limit of the available floating range and pushes the spring loaded pedal mechanism, increasing foot loads and creating additional stress to the knees (Ruby and Hull, 1993; Gregersen and Hull, 2003). Figures 4 b) and 4c) show the respective results for climbing in the sitting and standing position. The left foot shows large amplitudes that systematically exceed the range limit of the pedals (0-9°) for climbing.

5- Discussion

The goal of this work was to design an instrumented clipless pedal that would provide an accurate measurement of the floating angle under real operating conditions. Using commercial pedals to develop the instrument ensures normal use of the pedal floating in order to obtain realistic measurements. The use of a magnetic sensor also guaranteed that the pedal could be used safely because the cyclist is able to dismount easily if needed. Upon calibration, the direct sensitivity is very linear and consistent and the hysteresis is small.

A commercial clipless pedal is not an infinitely rigid structure and a slight deformation of the pedal body was observed when loads were applied. This was identified as the most important contributor to measurement error. Taking this fact into account, the influence of the pedal loading was measured and included in the measurement error.

Tolerance variations of the shape of the cleats do not allow an exact repositioning of the magnet on each cleat. It was found that the instrument's sensitivity is not significantly influenced by the variation in magnet position on the cleat. However, it may create a small angle measurement bias and zeroing is therefore required at each test to eliminate this bias.

The measurement principle is based on the evaluation of the direction of a magnetic field. The magnet placed very close to the sensor succeeds in generating a sufficiently strong magnetic field to yield measurements that are not influenced by the surroundings. For example, it was verified that the use of a steel bike or the earth's magnetic field did not influence the measurement. No significant drift was noted due to barometric pressure or temperature change.

No special effort was taken to make the instrument waterproof and consequently, it is not recommended for use in wet conditions. The apparatus requires small wires to be attached along the cyclist's legs. All of the cyclists tested stated they were not bothered by the wires.

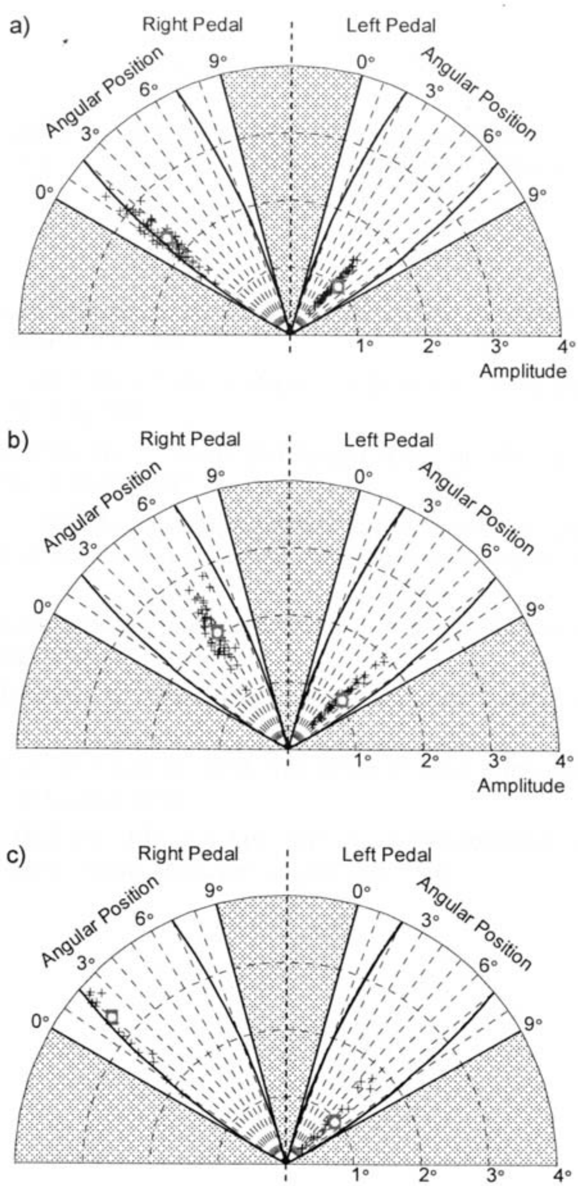

Figure 4 - Polar plot indicating the amplitude and position of the cleat for each cycle and for the left and right pedals; MA = Mean Amplitude; MP = Mean Position.
a) Flat road; Sitting; Number of cycles = 64; Left pedal: MA = 2.3°; MP = 1.4°; Right pedal: MA = 1.0°; MP = 5.2°
b) Climbing and sitting; Number of cycles = 48; Left pedal: MA = 2.1°; MP = 5.5°; Right pedal: MA = 1.0°; MP = 6.1°
c) Climbing and standing; Number of cycles = 20; Left pedal: MA = 3.4°; MP = 1.9°; Right pedal: MA = 0.9°; MP = 6.2°

6- Conclusion

Although measurements of very small angle variations in the field is a difficult task, the authors were able to demonstrate that the instrumented commercial pedal suitable for in-situ measurement of the floating angle used in these tests provides reliable and accurate results. No other instrument enabling the in-situ quantification of the floating angle of a commercial pedal has yet been reported. This quantification is useful to investigate the influence of power and cadence on the in-situ use (hill climbing, sitting position) of the floating angle. It is also useful for the development of cleat fitting techniques to optimize the use of clipless pedal floating.

7- Acknowledgments

The authors wish to thank ISAAC Instrument and LOOK Cycle International for their collaboration. This study received financial support from the National Sciences and Engineering Research Council of Canada (NSERC).

8- References

[BM1] Bailey, M.P., Maillardet F.J. and Messenger, N. Kinematics of cycling in relation to anterior knee pain and patellar tendinitis. Journal of Sports Sciences, 21:649-657, 2003.

[BN1] Boyd, T.F., Neptune, R.R. and Hull, M.L. Pedal and knee loads using a multi-degree-of-freedom pedal platform in cycling. Journal of Biomechanics, 30:505-511, 1997.

[EN1] Ericson, M.O., Nisell, R. and Ekholm, J. Varus and valgus loads on the knee joint during ergometer cycling. Scandinavian Journal of Sports Sciences, 6:39-45, 1984.

[GH1] Gregersen, C.S. and Hull, M.L. Non-driving intersegmental knee moments in cycling computed using a model that includes three-dimensional kinematics of the shank/foot and the effect of simplifying assumptions. Journal of Biomechanics, 36:803-813, 2003.

[RH1] Ruby, P. and Hull, M.L. Response of intersegmental knee loads to foot/pedal platform degrees of freedom in cycling. Journal of Biomechanics, 26:1327-1340, 1993.

[RH2] Ruby, P., Hull, M.L. and Hawkins, D. Three-dimensional knee joint loading during seated cycling. Journal of Biomechanics, 25:41-53, 1992.

[RH3] Ruby, P., Hull, M.L., Kirby, K.A. and Jenkins, D.W. The effect of lower-limb anatomy on knee loads during seated cycling. Journal of Biomechanics, 25:1195-1207, 1992.

[WH1] Wilber, C.A., Holland, G.J., Madison, R.E. and Loy, S.F. An epidemiological analysis of overuse injuries among recreational cyclists. International Journal of Sports Medicine, 16:201-206, 1995.